Modulation of Excited-State Proton-Transfer Reactions of 7-Hydroxy-4-methylcoumarin in Ionic and Nonionic Reverse Micelles

Sharmistha Dutta Choudhury[†] **and Haridas Pal***

Radiation & Photochemistry Division, Bhabha Atomic Research Centre, Trombay, Mumbai 400 085, India

Received: December 18, 2008; Revised Manuscript Received: February 28, 2009

The prototropic behavior of the dye, 7-hydroxy-4-methylcoumarin (7H4MC), has been studied in cationic benzyldimethylhexadecylammonium chloride (BDHC) and nonionic poly(oxyethylene)(tetramethylbutyl)phenyl ether (TritonX-100, TX-100) reverse micelles using ground-state absorption and steady-state and time-resolved fluorescence measurements. The results have been compared with the previous results in the anionic sodium 1,4-bis(2-ethylhexyl)sulfosuccinate (AOT) reverse micelles. Although the probe dye, 7H4MC, is indicated to reside in the interfacial region in all of the reverse micelles studied, significant differences have been observed in the evolution of the different prototropic species. In BDHC reverse micelles, the anionic form is favored over the tautomeric form at the higher w_0 values, which is contrary to the observation in AOT reverse micelles where both of these forms are almost equally produced. The higher propensity for the formation of the anionic form in BDHC reverse micelles has been explained on the basis of the additional electrostatic stabilization of the anionic species in the cationic BDHC reverse micelles compared to that in the anionic AOT reverse micelles. On the other hand, in TX-100 reverse micelles, the anionic form is not very evident, but interestingly, the tautomer form begins to appear beyond $w_0 = 2$. The appearance of the tautomeric species apparently coincides with the formation of the water pool in the TX-100 reverse micelles. However, due to the more restricted nature of the water molecules within this reverse micelle (mostly dispersed around the oxyethylene chains), deprotonation of the 7H4MC dye and the consequential stabilization of the anionic form are considerably reduced. The results clearly reveal that the aqueous environment in the vicinity of the probe is quite different for the reverse micelles considered, and these differences largely modulate the prototropic processes of the excited dye.

1. Introduction

In recent years, the quest for understanding of the nature of confined water in biological systems, for example, in the vicinity of DNA or in protein-binding pockets, has gained tremendous impetus. It is evident that water plays a major role in determining biomolecular structure and function, and it is becoming increasingly clear that the properties of biological water are vastly different from those of bulk water.[1–4] These differences primarily arise due to the confinement of water in small pockets and also due to the presence of localized charged boundaries. A systematic investigation of the structure and dynamics of water in biomolecules is a complex problem; hence, people usually resort to simple biomimicking organized assemblies to understand the behavior of confined water.[2,4] Among the variety of available organized molecular assemblies, reverse micelles constitute a good and extensively used alternative for such studies.

Reverse micelles are aggregates of surfactants dispersed in a nonpolar medium with their polar head groups oriented inward and the hydrocarbon chains oriented outward into the bulk nonpolar medium. Most of the investigations on reverse micelles have been carried out with those formed by ionic surfactants because of their ability to solubilize large amounts of water and to form well-defined water pools. The average size of such reverse micelles is dependent on the amount of solubilized water and can be expressed in terms of the water to surfactant molar ratio, $w_0 = [H_2O]/[\text{surfactant}]$.[5–8] Spectroscopic techniques, NMR, FTIR, as well as MD simulations show that not only are the properties of the water encapsulated inside of these reverse micelles markedly different from those of bulk water, but there also exist distinct water environments based on the distance from the surfactant interface.[8–14] At least two types of water populations are expected inside of the water pool, a shell of "bound" water molecules, which are strongly associated (by hydrogen bonding) with the polar head groups of the surfactants, and the "free" water molecules, which develop deep inside of the core of the water pool on increasing w_0, as the hydration of the surfactant polar head groups becomes saturated.[8] Upon increasing w_0, the extent of free water in a reverse micelle increases over the bound water. Moreover, the bound and free water not only just coexist but also exchange quite rapidly. Recent ultrafast infrared experiments by Fayer's group in the water nanopools of reverse micelles have revealed that the shell of water in the interfacial region has a different structure from that of the water present in the core.[13,14] The hydrogen bond network couples the water in the shell with the water in the core of the reverse micelles, and this coupled network has a distinctly slower dynamics compared to that in the bulk water.

The structure of water in the reverse micelles is of major importance for understanding the chemical reactivity of the dissolved solutes in these media. Studies on proton-transfer reactions in reverse micelles can provide interesting insights in this regard. Since the dynamics of proton transfer is dramatically affected by the ability of the solvent to reorganize and solvate the resulting ion pairs, proton-transfer reactions experienced by

* To whom correspondence should be addressed. E-mail: hpal@barc.gov.in. Fax: 91-22-25505151/25519613.
† E-mail: sharmidc@barc.gov.in.

10.1021/jp8111759 CCC: $40.75
Published on Web 04/17/2009

a suitable probe molecule can be a convenient reporter for the local environment in the aqueous interior of the reverse micelles.[15–20] Bardez et al. have investigated the localization of different excited-state proton donors such as 2-naphthol and sulfonated 2-naphthol derivatives in various regions of the reverse micelles formed by the anionic surfactant, sodium 1,4-bis(2-ethylhexyl)sulfosuccinate (AOT), and the corresponding ability of the microenvironments to accept a proton.[16] It was found that the charged photoacids like 2-naphthol sulfonato derivatives were localized within the water pool of the reverse micelles in the ground state and showed significant proton-transfer activity, whereas no deprotonation could be observed for 2-naphthol which is located in the relatively hydrophobic interface region, irrespective of the w_0 value. Further, Douhal et al. have observed that three different situations in the behavior of the confined water molecules within the reverse micelles can be realized using a proton-transfer probe.[20] The first situation is observed at w_0 values less than 2, where the shell of water bound to the surfactant head groups is mainly formed, and thus, the relaxation dynamics of these water molecules is dominated by the confinement effects. The second situation is observed at w_0 values from 2 to 5, where the core (water pool) of the reverse micelle gradually grows with an increase in its water content and accordingly changes the relaxation dynamics of these water molecules. The third situation arises beyond $w_0 = 5$, where the water pool is already fully grown, and thus, there is no further change in the observed relaxation dynamics.

Recently, we have studied the excited-state proton-transfer and phototautomerizaton behavior of 7-hydroxy-4-methylcoumarin (7H4MC) dye in AOT reverse micelles.[21] The dye displays interesting excited-state proton-transfer behavior and complex pH-dependent fluorescence properties.[22–38] In the ground state, 7H4MC is mildly acidic ($pK_a \sim 7.7$), but upon photoexcitation, its acidity increases sharply ($pK_a^* \sim 0.45$).[22–25] Depending on the solvent and pH, multiple fluorescence spectra can be observed for 7H4MC, corresponding to its excited neutral (N*, ~380 nm), anionic (A^{*-}, ~450 nm), cationic (C^{*+}, ~412 nm), and tautomeric (T*, ~490 nm) forms.[22,23,31] In the ground state, however, only the neutral, cationic, and anionic forms of the dye can be identified at suitable pH conditions. The tautomeric form is an excited-state reaction product and arises due to proton transfer between the spatially separated acidic (OH) and basic (C═O) groups of 7H4MC. The prototropic transformations of 7H4MC have been quite extensively studied in aqueous ethanolic solutions[22,23,32–37] and in the presence of β-cyclodextrin hosts.[38] The phototautomerization process in the excited 7H4MC dye has been suggested to take place either through "dissociative" two-step pathways[34,37] involving the anionic or cationic species as the intermediates or through a "nondissociative" one-step concerted proton-transfer reaction[22,23] from the hydroxyl to the carbonyl site via hydrogen-bonded solvent molecules. The different prototropic transformations that may be possible in 7H4MC dye are generally presented by a unified Scheme 1. In our studies using AOT reverse micelles, only the neutral form of the dye has been observed both in the ground and the excited states at $w_0 = 0$, whereas at higher w_0 values, three prototropic forms, namely, neutral, anionic, and tautomeric, have been identified in the excited state, although only the neutral form of the dye is present in the ground state (pH ~ 5).[21] In bulk water, however, there is no evidence of the tautomeric species, and only the anionic form is observed in the excited state under similar pH conditions. The observed results in AOT reverse micelles indicate that the anionic and tautomeric forms of the dye are excited-state reaction products and arise apparently independently from the same population of the excited neutral form of the dye solubilized at the interfacial region of the reverse micelles.

SCHEME 1: General Reaction Scheme for the Photoexcited States of 7H4MC[a]

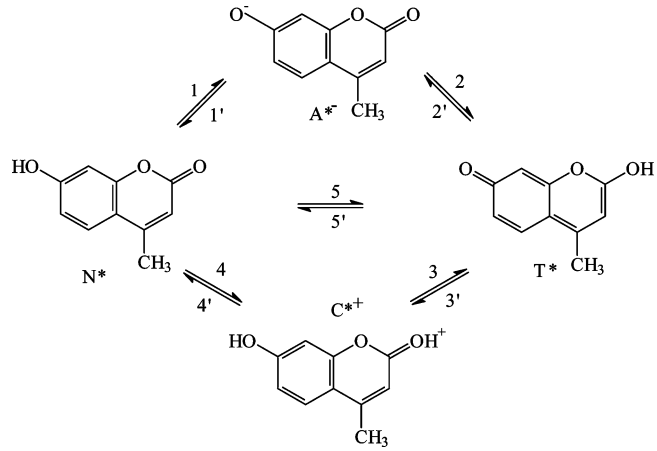

[a] N*, A^{*-}, C^{*+}, and T* represent the excited states of the neutral, anionic, cationic, and the tautomeric forms.

CHART 1: Chemical Structures of the Surfactants (I) TX-100 and (II) BDHC

(I) $CH_3C(CH_3)_2CH_2C(CH_3)_2C_6H_4(OCH_2CH_2-)_{9.5}OH$

poly(oxyethylene)(tetramethylbutyl)phenyl ether, TX-100

(II) $CH_3(CH_2)_{15}N^+(CH_3)_2(CH_2C_6H_5)\ Cl^-$

benzyldimethylhexadecylammonium chloride, BDHC

In the present work, we have extended our studies on the prototropic behavior of the same dye, 7H4MC, to investigate the aqueous interior of two other reverse micelles formed by surfactants with cationic and nonionic head groups, in comparison to the anionic AOT. The surfactant, benzyldimethylhexadecylammonium chloride (BDHC) in benzene was chosen as the cationic reverse micelle system, and the surfactant poly(oxyethylene)(tetramethylbutyl)phenyl ether (TritonX-100, TX-100) in a mixed solvent of benzene and *n*-hexane (30:70, v/v) was chosen as the nonionic reverse micelle system. Using this mixed solvent composition, an optimum combination of large hydrodynamic radius of the dry reverse micelle and a wider range of w_0 can be reached at a small surfactant concentration.[39] The structures of these surfactants are show in Chart 1. The BDHC/benzene/water reverse micelle system has properties similar to those reported for the AOT reverse micelle, especially in terms of solubilizing large amounts of water and in relation to the "free" and "bound" water molecules in the water pool.[12,40–42] On the other hand, the reverse micelles formed by the nonionic surfactant TX-100 are structurally very different.[39,43,44] Unlike the ionic surfactants which have a localized polar head group, nonionic surfactants possess an extended hydrophilic region. In TX-100, the hydrophilic oxyethylene chain, with an average of 9.5 units, is longer than the hydrophobic part. The added water hydrates and remains dispersed between the oxyethylene chains of the surfactants. The amount of water that can be solubilized in these reverse micelles is also significantly low compared to that in ionic reverse micelles. In the TX-100/benzene−hexane/water system, phase separation occurs beyond $w_0 \sim 9.5$. Moreover, contrary to the reverse micelles formed

by ionic surfactants, which have roughly spherical and well-defined water pools, the nature of water present in nonionic reverse micelles is not very well understood. Further, the size of these reverse micelles cannot be expressed clearly in terms of the w_0 values.[39] The differences in the confined water pools of the various reverse micelles have been explored in this work by following the prototropic behavior of the dye 7H4MC using ground-state absorption and the steady-state and time-resolved fluorescence measurements.

2. Materials and Methods Section

The coumarin dye, 7H4MC, was obtained from Schuchardt München and was purified by recrystallization from acetonitrile. The surfactant, TX-100, was obtained from Riedel-de-Haën, and BDHC was obtained from Fluka. The spectroscopic-grade solvents benzene and *n*-hexane were obtained from Spectrochem (India) and were used without further purification. Nanopure water with a conductivity of less than 0.1 μS cm^{-1} was obtained from a Millipore Elix-3/A10 water purification system and was systematically added, after suitable pH adjustment, to prepare reverse micelle solutions with desired w_0 values. The TX-100 and BDHC concentrations were kept at 0.27 M, and the concentration of 7H4MC was maintained in the range of $10^{-5}-10^{-6}$ M. Freshly prepared solutions were always used throughout the present study.

The absorption spectra were recorded on a Shimadzu UV−vis spectrophotometer (model UV-160A), and steady-state fluorescence spectra were recorded on a Hitachi spectrofluorimeter (F-4010). All of the reported fluorescence spectra are corrected for the wavelength-dependent responses of the instrument. The time-resolved fluorescence measurements were carried out using a time-correlated single-photon counting (TCSPC) spectrometer (Edinburgh Instruments, Model 199). A hydrogen-filled coaxial flash lamp having a pulse duration around 1 ns (fwhm) was used as the excitation source. The fluorescence decay curves were analyzed by a reconvolution procedure using a proper instrument response function, obtained by substituting the sample cell with a light scatterer. The decay curves were fitted by considering either single-exponential or multi-exponential decay functions. The quality of the fits was judged from the reduced chi-square (χ_r^2) values and the distribution of the weighted residuals among the data channels. For all of the accepted fits, the χ_r^2 values were close to unity, and the distribution of the weighted residuals were quite random among the data channels.[45,46]

3. Results and Discussion

3.1. Absorption and Fluorescence Spectral Features and Time-Resolved Fluorescence Parameters of 7H4MC in Cationic BDHC Reverse Micelles. Figure 1 shows the absorption spectra of 7H4MC in water and in BDHC reverse micelles at different w_0 values. In all cases, only the neutral form of the dye is observed with a maximum at around 320 nm in water[22] and at around 326 nm in BDHC reverse micelles. The slight red shift for the spectra in BDHC reverse micelles as compared to that in water is similar to that observed in AOT reverse micelles and has been attributed to the greater stabilization of the π-electron system of 7H4MC in the ground state than in the excited state by the specific hydrogen-bonding interactions.[22] No significant spectral changes are observed upon addition of water to the dry ($w_0 = 0$) reverse micelles. Since the solubility of 7H4MC in benzene is unusually low and it is enhanced significantly in the presence of BDHC, it may be expected that

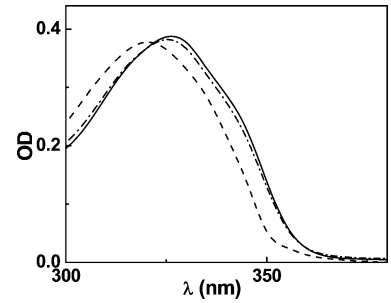

Figure 1. Absorption spectra of 7H4MC in water at pH 2 (− − −) and in BDHC reverse micelles with $w_0 = 0$ (—) and 20 (− • − • − •).

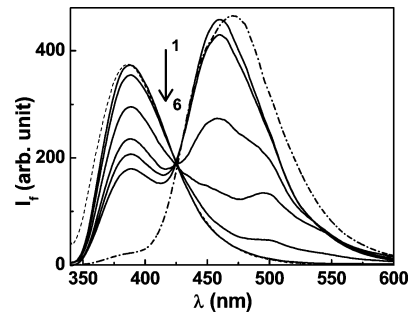

Figure 2. Fluorescence spectra of 7H4MC in benzene (− − −), water (− • − • − •) and in BDHC reverse micelles with w_0 = (1) 0, (2) 2, (3) 5, (4) 10, (5) 20, and (6) 30, upon excitation at 320 nm.

7H4MC resides mainly at the interfacial region (head group region) of the reverse micelles toward the water pool. It may be mentioned here that the ground-state pK_a of 7H4MC is reported to be around 7.7,[22,24] so that at pH values < 7.7, the neutral form of the dye with an absorption maximum at 320 nm will be predominantly observed, and at pH values > 7.7, the anionic form of 7H4MC with an absorption maximum at 360 nm will be observed in water. However, in BDHC reverse micelles, due to the cationic charge of the BDHC head groups, the pK_a of the dye in the interfacial region is expected to be significantly affected, so that at pH values above 2, the anionic form of the dye can be detected by a hump in the absorption spectrum at around 360 nm. Hence, for the present study in BDHC reverse micelles, the pH of water was maintained at ∼2 to ensure that there is no preexistence of the anionic form of 7H4MC in the micellar solution.

The fluorescence spectra of 7H4MC in BDHC reverse micelles at different w_0 values are presented in Figure 2. In the dry BDHC reverse micelles, a single emission peak is observed with a maximum at around 387 nm, which corresponds to the emission from the excited neutral form (N*) of the dye.[22,23,31] Upon successive addition of water, the emission from the neutral form at 387 nm decreases with a concomitant increase in the emission at higher-wavelength regions along with the appearance of an isoemissive point at 425 nm. It is interesting to note that the emission band for the excited neutral form of the dye in BDHC reverse micelles is almost similar to that in the pure solvent benzene, except that the band is marginally red-shifted in the former case (cf. Figure 2). This observation in addition to the fact that the solubility of the dye increases substantially in reverse micelles in comparison to that in pure benzene supports our assumption that the dye preferentially resides at the interfacial region of the reverse micelles. Due to very low solubility of 7H4MC in pure benzene, the fluorescence intensity observed in this solvent was unusually weak compared to that in reverse micelle. For clarity of presentation, the fluorescence

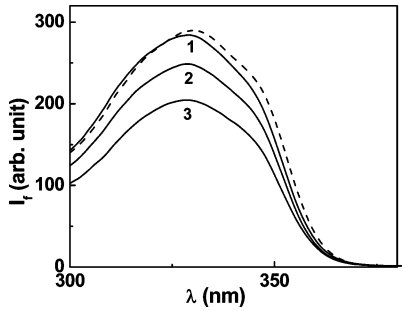

Figure 3. Excitation spectra of 7H4MC in BDHC reverse micelles at $w_0 = 0$ monitored for 380 nm emission (− − −) and at $w_0 = 20$ monitored for (1) 380, (2) 460, and (3) 500 nm emission.

spectrum of 7H4MC in benzene was normalized to that in dry BDHC reverse micelle, as shown in Figure 2.

At lower w_0 values, in addition to the emission at 387 nm, a hump at around 500 nm is clearly discernible, which is ascribed to the emission from the tautomer (T*) form of the dye, resulting from the excited-state intramolecular proton transfer (ESIPT) in N*.[22,23] On the other hand, at higher w_0 values, the tautomer emission is superseded by the emission from the anionic form (A^{*-}), and the emission maximum appears at around 460 nm. It may be noted that this 460 nm emission band observed in the present cases appears to be somewhat red-shifted compared to the emission maximum of ~450 nm for the pure anionic form observed in neutral water. This is possibly due to the overlap of the tautomer emission band, which causes the apparent emission maximum to be somewhat red-shifted compared to that of the pure anion emission peak. The emission spectrum of 7H4MC in pure water at pH ~ 2 is also shown in Figure 2 for comparison. In this case also, the emission band is mainly due to the anionic form, but the emission peak appears at around 470 nm, which is again somewhat red-shifted in comparison to the 450 nm peak for the anion emission observed in neutral water. This is also ascribed to the overlapping emissions from the anionic and the tautomer forms of the dye in the acidic aqueous solutions, as reported in an earlier study.[36] It may be noted from Figure 2 that the emission spectrum of 7H4MC in BDHC reverse micelles at the highest w_0 value used ($w_0 = 30$) is still quite different from that observed in aqueous solution. This indicates that the aqueous environment in the vicinity of the probe is considerably different compared to that in bulk water. At this high w_0 value, it is expected that the nature of the water at the core of the water pool in the reverse micelle will be quite similar to that in bulk water. Thus, the present observation suggests that in the present cases, the dye 7H4MC mainly resides at the interfacial region rather than solubilizing in the core of the reverse micelles.

From the absorption and fluorescence spectral changes, it is obvious that both the anionic and tautomeric species are the excited-state reaction products since there is no evidence of these forms in the absorption spectra of 7H4MC in BDHC reverse micelles. The excitation spectra of the dye in BDHC reverse micelles at different w_0 values recorded at emission wavelengths of 380, 460, and 500 nm (Figure 3) show only one peak at around 326 nm corresponding to the neutral form of 7H4MC, which further confirms that the neutral form is exclusively present in the ground state. Moreover, the appearance of an isoemissive point in the emission spectra suggests that the anionic and the tautomeric forms arise concurrently from the excited neutral form of the dye, as has been indicated from our previous study in AOT reverse micelles.[21] It may be noted that since the proton-donating group (OH) and the proton-accepting group (C═O) of 7H4MC are spatially separated, a direct transfer of the proton in the excited neutral from of the dye to produce its tautomer form is not possible, and the transfer has to take place through a solvent bridge between the OH and the C═O group of the dye. Very recently, Georgieva et al. have reported, using theoretical calculations, that the excited-state proton transfer in 7H4MC can take place along a hydrogen-bonded water wire of three water molecules bridging the proton-donor and the proton-acceptor groups.[30] Thus, following the suggestion of Georgieva et al., it is expected that even at the relatively lower w_0 values, there are sufficient water molecules present at the interfacial region of the reverse micelles to bridge the OH and the C═O groups of 7H4MC dye.

Although the fluorescence spectral changes of 7H4MC upon increasing w_0 in BDHC reverse micelles are qualitatively similar in many respects with those in AOT reverse micelles, especially regarding the evolution of the anionic and the tautomer emissions and the observation of an isosbestic point, there are some distinct differences between the two systems that clearly indicate the effect of the different charge characteristics of the surfactant head groups in the AOT and BDHC reverse micelles. In AOT reverse micelles, both the anionic and tautomer emissions were found to evolve simultaneously and maintain the same intensity ratios at all of the w_0 values studied. On the contrary, in BDHC reverse micelles, the intensity of the emission from the anionic form gradually exceeds that of the tautomer emission upon increasing the w_0 value, and at the higher w_0 values, the tautomer emission is completely buried within the emission band of the anionic form. At low w_0 values, most of the water molecules in the aqueous pool of the reverse micelles are supposed to exist at the interfacial region as the "bound" water molecules to the surfactant head groups by hydrogen-bonding interactions. Thus, at low w_0 values, as the availability of the free water molecules or water molecules having a partially broken hydrogen-bonded network structure present in the reverse micelle is very limited, the stabilization of the anionic form of the dye cannot dominate over the tautomer form of the dye. However, at higher w_0 values, when the amount of free water substantially increases, the anionic forms can be preferentially stabilized to a large extent due their solvation. Moreover, since 7H4MC resides in the interfacial region, the anionic form of the dye experiences additional electrostatic stabilization in the cationic BDHC reverse micelles compared to that in the anionic AOT reverse micelles. The combination of these effects favors the conversion of the excited neutral form of the dye to its anionic from compared to its conversion to the tautomer form. Accordingly, there is a greater emission from the anionic form of the dye compared to its tautomeric form at higher w_0 values of BDHC reverse micelles.

To have a better idea about the different emissive species present in the BDHC reverse micelles and to understand the correlation and interconversion between them, the fluorescence lifetimes for the different prototropic forms of the dye were measured at 380, 460, and 500 nm at different w_0 values. Representative decay traces are shown in Figure 4, and the decay parameters are presented in Table 1. It is clearly seen that upon increasing w_0, the lifetime of the neutral species (~380 nm) gradually decreases due to the participation of the processes that lead to the formation of the anionic and the tautomeric species of the excited dye. The single-exponential decay of the neutral form, however, indicates that the back reactions from the excited anionic and tautomeric forms to the excited neutral form are either negligible or not occurring at all within the time

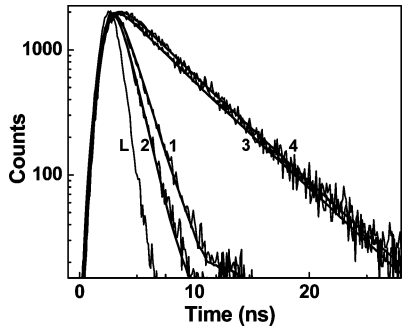

Figure 4. Time-resolved fluorescence decays of 7H4MC in BDHC reverse micelles monitored at (1) 380 nm, $w_0 = 0$, (2) 380 nm, $w_0 = 20$, (3) 460 nm, $w_0 = 20$, and (4) 500 nm, $w_0 = 20$. L is the instrument response function. The excitation wavelength was 320 nm in all cases.

resolution (1 ns) of the present instrument. The fluorescence decay at 460 nm (emission peak for the anionic form) is biexponential in nature at the lower w_0 values, with a short lifetime component similar to that of the neutral form of 7H4MC and a longer lifetime component possibly corresponding to the decay time of the anionic form of the dye. The biexponential nature in these cases thus arises mainly due to the overlapping emission of the neutral and the anionic forms at the lower w_0 values. At the higher w_0 values, however, the decay traces at 460 nm can essentially be fitted to a single-exponential function with a decay time of about 4.7 ns, attributed to the lifetime of the anionic species. Ideally, a growth component corresponding to the formation of the anionic form from the excited neutral form should also have been observed for the fluorescent transient measured at 460 nm. However, in reality, it could not be resolved in the present study possibly due to the large overlapping of the emissions around this wavelength region from the different emissive species in the system. As expected, a growth component, however, could be undoubtedly observed for the fluorescent transient measured at 500 nm, which effectively corresponds to the decay of the neutral form of 7H4MC at 380 nm. This further supports that the tautomer emission at ~500 nm arises from the excited neutral form. It may be noted that a decrease in the growth component is apparently indicated at higher w_0 values. This is in accordance with the fact that at higher w_0 values, the emission from the anionic form dominates over the tautomeric form of the dye in the BDHC reverse micelles. Recently, Giestas et al. have studied the kinetics of the excited-state proton-transfer processes of a photoacid present at the surface of a micelle.[47] In their study, the system is relatively simplified because it involves only a single acid−base equilibrium. In the present case, the involvement of two simultaneous equilibria coupling the anionic and the tautomer species with the excited neutral form makes the overall kinetic processes very complicated. Moreover, strong overlap of the emission spectra of the different species at the measuring wavelengths as well as the limited time resolution of the present experimental setup makes it practically impossible to carry out a detailed kinetic analysis for the formation of the anionic and the tautomeric species of the dye from the excited neutral dye molecules in BDHC reverse micelles. However, the observed time-resolved results in the present systems apparently indicate that the fluorescence lifetimes of both anionic and tautomeric forms of the dye are almost in the similar range, ~4.6−4.8 ns (cf. Table 1). de Melo and Maçanita have reported a detailed study using picosecond time resolution on the photokinetic triangle involving the coupling of the three excited-state species, namely, the neutral, anionic, and tautomer forms of 7H4MC, in dioxane−water mixed solvent and thus obtained the estimations of the different rate constants involved in the kinetic scheme.[32] From their study, the estimates for the fluorescence lifetimes of the neutral, anionic, and tautomeric forms of 7H4MC dye in dioxane−water mixed solvent are obtained as 2.60, 5.20, and 5.45 ns, respectively. Though these values are somewhat higher than the corresponding values estimated in the present cases in BDHC reverse micelles, these results clearly indicate that the lifetimes of the anionic and the tautomeric forms of 7H4MC dye are quite similar to each other, as also observed in the present study.

3.2. Absorption and Fluorescence Spectral Features and Time-Resolved Fluorescence Parameters of 7H4MC in Nonionic TX-100 Reverse Micelles. Figure 5 shows the absorption spectra of 7H4MC in TX-100 reverse micelles at different w_0 values and in water at similar pH conditions (pH ~5). In the dry reverse micelles, in addition to the main absorption band at ~324 nm, a hump is also observed at around 370 nm. Upon addition of water to the dry TX-100 reverse micelles, surprisingly, the absorbance in the higher-wavelength region decreases while the absorption at ~320 nm increases. As mentioned earlier, the neutral form of 7H4MC dye has an absorption maximum at around 320 nm, and the anionic form has a maximum absorption at around 360 nm. However, the 370 nm band in TX-100 reverse micelles cannot be unambiguously assigned to the anionic form of the dye because, contrary to our expectation, the absorbance of this band decreases with the addition of water in TX-100 reverse micelles. Moreover, in the present case, the 370 nm hump was also observed even at the lower pH values, up to pH ~2. Therefore, it is evident that the absorption in the 370 nm region cannot be due to the anionic form of the dye. It may be mentioned here that since no further changes were observed in the absorption spectra of 7H4MC in TX-100 reverse micelles beyond pH 5, further experiments in this reverse micelle were performed at pH 5. The slightly lower pH (~5) than the pK_a value of the dye was chosen in this case to ensure that there is no preexistence of the anionic form of the dye in solution.

Since the 370 nm absorption band cannot be assigned to the anionic form of the dye, the development of this band undoubtedly suggests that there is a kind of specific interaction for 7H4MC dye with the surfactant head groups. Previously, Andrade et al. have observed a Lewis base character of TX-100 in the interaction with another dye, acridine orange.[48] In the present case also, it is possible that TX-100 acts as a Lewis base toward 7H4MC, and thus, a part of the dye molecules form a kind of contact ion pair ($7H4MC^{\delta-}/TX\text{-}100^{\delta+}$, I) at the interfacial region, which absorbs in the longer-wavelength region (~370 nm). Such an ion pair formation with a corresponding absorption band in the longer-wavelength region has also been reported for 7H4MC dye with the bases like triethyl amine in some nonhydroxylic solvents.[23] Along with the contact ion pairs, the major part of the dye in TX-100 reverse micelles exists in its neutral form and corresponds to the absorption band at around 324 nm. It is possible that the neutral form of the dye in dry TX-100 reverse micelles undergoes some kind of intermolecular hydrogen-bonding interaction with the surfactant head groups which stabilizes the ground state of the dye and leads to a small red shift in the absorption band (~324 nm) in comparison to that observed at higher w_0 values (~320 nm). It is expected that with increasing w_0, there will be a competition between the water molecules and the dye molecule for the interaction with the TX-100 head groups. Thus, there will be a gradual conversion of the hydrogen-bonded complexes to the free neutral

TABLE 1: Time-Resolved Decay Parameters[a] of 7H4MC at Different Emission Wavelengths in BDHC Reverse Micelles with Varying w_0 Values upon Excitation at 320 nm[b]

	380 nm		460 nm				500 nm			
w_0	A_1 (%)	τ_1 (ns)	A_1 (%)	τ_1 (ns)	A_2 (%)	τ_2 (ns)	A_1 (%)	τ_1 (ns)	A_2 (%)	τ_2 (ns)
0	100	1.4								
2	100	1.3	36	3.1	64	1.3	102	4.6	−2	1.2
5	100	1.2	52	4.3	48	1.2	109	4.7	−9	1.1
10	100	1.1	90	4.6	10	1.1	111	4.5	−11	1.0
20	100	1.0	100	4.7			110	4.5	−10	1.0
30	100	0.9	100	4.8			108	4.7	−8	1.0

[a] The intensity decays were fitted according to $I(t) = \sum_i a_i \exp(-t/\tau_i)$ for single and biexponential decays; χ_r^2 values in all cases are close to 1. [b] A_1 and A_2 correspond to the relative contributions[c] of the two lifetimes, τ_1 and τ_2, in the case of biexponential decays. [c] The relative contributions were estimated as $A_i = (a_i\tau_i)/(\sum_i a_i\tau_i)$. The relative contribution of the growth component is apparently lower due to the shorter time constant (~1.0 ns) of this component compared to that of the decay component (~4.7 ns).

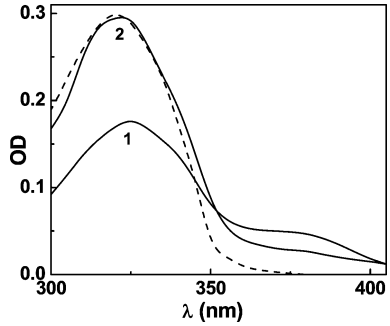

Figure 5. Absorption spectra of 7H4MC in water at pH 5 (− − −) and in TX-100 reverse micelles with w_0 = (1) 0 and (2) 6.

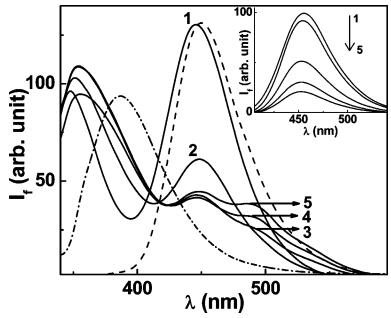

Figure 6. Fluorescence spectra of 7H4MC in the benzene−hexane solvent mixture (− • − • − •), water (− − −), and TX-100 reverse micelles with w_0 = (1) 0, (2) 1, (3) 2, (4) 4, and (5) 6 upon excitation at 320 nm. The inset shows the fluorescence spectra for the same system (1−5) upon excitation at 370 nm.

form of the dye, causing the 324 nm band for the neutral dye to shift gradually toward 320 nm. Moreover, with an increasing w_0 value, as the oxyethylene chains of TX-100 gradually become hydrated, its Lewis base character gradually decreases, and thus, the formation of the contact ion pairs by the interaction between the dye and the TX-100 head group ($7H4MC^{\delta-}/TX\text{-}100^{\delta+}$) gradually becomes disfavored. Therefore, with increasing w_0, there is an effective decrease in the absorbance at the longer-wavelength region (370 nm) with a concomitant increase in the absorbance at around 320 nm.

The fluorescence spectra of 7H4MC in the TX-100 reverse micelles at different w_0 values, upon excitation at 320 nm, are shown in Figure 6. The emission spectra of the dye in the benzene−hexane solvent mixture (normalized with respect to the fluorescence intensity in the dry TX-100 reverse micelles) as well as those in water at pH 5 are also shown in Figure 6 for comparison. In the dry reverse micelles, two emission bands are observed, one at around 350 nm and the other at around 445 nm. At w_0 = 1, the lower-wavelength emission band becomes broader and is red-shifted while the 445 nm emission band shows a considerable decrease in intensity. At higher w_0 values, the lower-wavelength emission band is further broadened and more red-shifted, the 445 nm emission band decreases in its intensity and apparently saturates to a limiting value, and, concomitantly, a new emission band develops at around 490 nm for which the intensity gradually increases with w_0. It may be mentioned that beyond w_0 = 6 and up to the phase separation limit of the present microheterogeneous system, there is no further significant change in the observed emission spectra of 7H4MC in TX-100 reverse micelles.

From our previous studies and also from the literature reports, the long-wavelength emission band at ~490 nm, which starts appearing above w_0 = 2, can be assigned to the tautomer emission (T*) of the dye. The emission at 350 nm in the dry reverse micelle is tentatively assigned to that of a hydrogen-bonded complex of the neutral dye molecule with the TX-100 head group. The broadening and the red shift of this lower-wavelength emission band with increasing w_0 can thus be explained in terms of the gradual conversion of the hydrogen-bonded complexes to the free neutral form of the dye upon addition of water due to the increased hydration of the TX-100 head groups at higher w_0 values. It may be noted that the free neutral form in the benzene−hexane solvent mixture emits at around 370 nm.

The emission at 445 nm is assigned to the emission from the excited contact ion pair (I*) as this band arises even in the dry TX-100 reverse micelle, and the formation of the contact ion pair, I, in the ground state is indicated from the absorption spectra (cf. Figure 5). This is further supported by the fact that upon excitation at 370 nm (corresponding to the absorption band of I), a clear single emission band is observed with a maximum at around 450 nm (inset, Figure 6). The slightly blue-shifted emission (~445 nm) observed upon excitation at 320 nm could be due to the overlapping of the emissions from the neutral and the hydrogen-bonded complexes of 7H4MC (cf. Figure 6). With increasing w_0, concomitant with the decrease in the absorbance for the 370 nm band (cf. Figure 5), the emission intensity for the 450 nm band is also seen to decrease upon exciting the system at 370 nm. Thus, we infer that with increasing w_0 due to the increased hydration of the oxythylene chains, the contact ion pairs between the dye and TX-100 are disrupted, leading to a reduction in the intensity for the 445 nm emission band (cf. Figure 6). It should be mentioned, however, that along with the emission from the excited ion pair, I*, some additional contribution from the emission of the anionic species (A^{*-}) formed by the excited-state proton transfer of the excited neutral dye to the medium cannot be ruled out for the emission band observed at around 445 nm, especially at

higher w_0 values. In fact, the saturation of the 445 nm emission band beyond $w_0 \sim 3$ possibly suggests that at these higher w_0 values, the anionic species, A^{*-}, in fact contributes to some extent at the emission band at around 445 nm. Nevertheless, the deprotonation of 7H4MC in TX-100 reverse micelles seems to be much less favored as compared to that in BDHC and AOT reverse micelles. Thus, contrary to the observation in the cationic BDHC reverse micelles and the anionic AOT reverse micelles, the anionic form of 7H4MC is not seen to increase that significantly in the nonionic TX-100 reverse micelles with an increase in the w_0 value. These interesting differences among the reverse micelles cannot be simply attributed to the charge characteristics of the surfactant head groups since the anionic form of 7H4MC is quite distinctly observed both in the anionic AOT reverse micelles and in the cationic BDHC reverse micelles.

As in the other reverse micelles, in TX-100 reverse micelles also, the dye is expected to reside in the interfacial region. The prototropic behavior of the dye clearly indicates that the water structure in the vicinity of the probe is considerably different from that of bulk water even at the highest w_0 value. Possibly, the anionic form of 7H4MC cannot stabilize significantly in TX-100 reverse micelles due to the more restricted nature of the interfacial water in this reverse micelle compared to that in ionic reverse micelles like AOT and BDHC. Interestingly, however, the tautomer emission is very clearly observed in TX-100 reverse micelles beyond $w_0 = 2$. Zhu et al. have reported that in TX-100/benzene−hexane/water reverse micelles, the added water first hydrates the oxyethylene chains of TX-100, and then, water pool formation starts in the range of $w_0 = 2-2.5$.[43] Therefore, the appearance of the tautomer emission beyond $w_0 = 2$ nicely coincides with this proposition of the formation of the water pool in the TX-100 reverse micelles. This suggests that as the hydration of the oxyethylene chains of the surfactants becomes almost saturated, sufficient water molecules become available to reorient themselves around the dye to form a hydrogen-bonded bridge between the hydroxyl and the carbonyl groups of 7H4MC, so that the excited-state intramolecular proton-transfer (ESIPT) process can occur to form the tautomeric species. However, in TX-100 reverse micelles, the water pool in the micellar core is expected to be quite small and not that well-defined as in other reverse micelles as most of the water molecules will mainly be dispersed in between the long hydrophilic oxyethylene chains of the surfactant moelecules. As a result, the ability of this dispersed water to accept a proton and consequently to solvate the resulting dye anion will be considerably less pronounced in TX-100 reverse micelles. Accordingly, the anionic form of 7H4MC is not appreciably formed in this reverse micelle system.

That the emission band observed at 455 nm arises mainly due to emission from the contact ion pair (I*) whereas the tautomer emission arises due to excited-state intramolecular proton transfer (ESIPT) in the excited neutral dye can be understood by examining the excitation spectra of 7H4MC recorded for different emission wavelengths in the TX-100 reverse micelle systems. The excitation spectra of 7H4MC monitored for the 445 nm emission band in the dry TX-100 reverse micelle shows two peaks at ~345 and ~375 nm (Figure 7). Upon addition of water, the 375 nm band decreases while the 345 nm band increases in intensity. The prominent appearance of the 375 nm band in the excitation spectra, however, is a clear indication that the 445 nm emission band arises due to the excitation of the contact ion pair, I, formed between TX-100 and 7H4MC in the ground state. When monitored at 490 nm (corresponding to the tautomer emission, T*), the excitation spectra of 7H4MC in TX-100 reverse micelles at $w_0 = 0$ and 1 match those monitored for the 445 nm emission band, with peaks observed at ~345 and ~375 nm. However, at higher w_0 values, the intensity of the hump at 375 nm is significantly lowered, and the peak on the blue side shifts to ~328 nm (Figure 7). This suggests that the tautomer form arises from the excited neutral dye due to an ESIPT process. The markedly red-shifted excitation peak at ~345 nm observed in the excitation spectra of 7H4MC (in comparison to the absorption maxima observed at ~324 nm) at the lower w_0 values for both the 450 and 490 nm emission bands could be due to the overlapping emissions from different prototropic and hydrogen-bonded forms of the dye in these spectral regions.

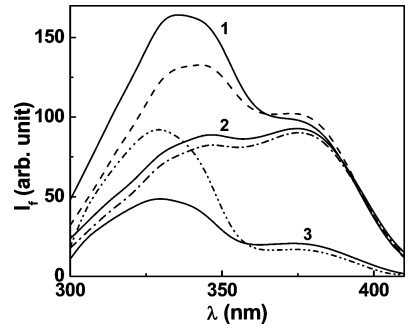

Figure 7. Excitation spectra of 7H4MC in TX-100 reverse micelles monitored for the 445 nm emission at $w_0 = (1)$ 0, (2) 1, and (3) 6 and for the 490 nm emission at $w_0 = 0$ (− − −), 1 (− • − • − •), and 6 (− • • − • • − • •).

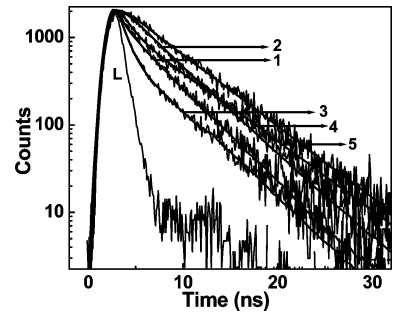

Figure 8. Time-resolved fluorescence decays of 7H4MC in TX-100 reverse micelles monitored at (1) 350 nm, $w_0 = 0$, (2) 450 nm, $w_0 = 0$, (3) 370 nm, $w_0 = 6$, (4) 450 nm, $w_0 = 6$, and (5) 490 nm, $w_0 = 6$. L is the instrument response function. The excitation wavelength was 320 nm in all cases.

To obtain information on the dynamics of the ESPT process, the fluorescence decays of 7H4MC in TX-100 reverse micelles were monitored at 370 (350 for the dry reverse micelle), 450, and 490 nm at different w_0 values (Figure 8, Table 2). In the dry TX-100 reverse micelles, the fluorescence decay of 7H4MC at 350 nm was biexponential in nature with two lifetimes, 3.7 and 0.4 ns, whereas at 450 and 490 nm, the fluorescence decays were effectively single-exponential with lifetimes of ~4.2 ns and ~4.8 ns, respectively. With increasing w_0, there was an increase in the contribution of the fast lifetime component for the fluorescence decay of 7H4MC monitored at 370 nm. In addition, the fluorescence decay at 450 nm became biexponential in nature with an increasing contribution of a fast lifetime component, ~0.8 ns, along with the long lifetime component, ~5 ns. However, the lifetime values remained more or less similar at all of the higher w_0 values for the transients at 370 and 450 nm. Unlike the fluorescence decays observed in the AOT and BDHC reverse micelles, a gradual decrease in the

TABLE 2: Time-Resolved Decay Parameters[a] of 7H4MC at Different Emission Wavelengths in TX-100 Reverse Micelles with Varying w_0 Values upon Excitation at 320 nm[b]

	350/370 nm				450 nm				490 nm			
w_0	A_1 (%)	τ_1 (ns)	A_2 (%)	τ_2 (ns)	A_1 (%)	τ_1 (ns)	A_2 (%)	τ_2 (ns)	A_1 (%)	τ_1 (ns)	A_2 (%)	τ_2 (ns)
0	88	3.9	12	0.2	100	4.2			100	4.8		
1	60	3.8	40	0.5	93	4.7	7	0.7	100	4.9		
2	45	3.8	55	0.6	82	5.1	18	0.7	105	4.9	−5	0.5
4	50	3.7	50	0.6	79	5.2	21	0.9	105	4.9	−5	0.4
6	52	3.9	48	0.5	80	5.3	20	0.9	110	5.0	−10	0.4

[a] As defined in the footnote of Table 1. The relative contribution of the growth component is apparently lower due to the shorter time constant (∼0.4 ns) of this component compared to that of the decay component (∼5 ns). [b] A_1 and A_2 correspond to the relative contributions[a] of the two lifetimes, τ_1 and τ_2, in the case of biexponential decays.

lifetime of the neutral form at 370 nm was not observed in TX-100 reverse micelles. Since the absorption and fluorescence spectral data indicate the existence of different hydrogen-bonded forms and a contact ion pair state of 7H4MC with the TX-100 head group, the observed time constants could not be assigned clearly to any of the emissive species. Probably, the two decay times in the 350−370 nm wavelength regions correspond to the free and the hydrogen-bonded forms of the dye. The biexponential nature of the decay at 450 nm with increasing w_0 is possibly due to the increasing overlap of the emissions from the free dye (due to broadening and red shift of the 350/370 nm band) and the excited ion pair state (and/or anion). It may be mentioned that upon excitation at 370 nm, only one emission band was observed with a maximum at around 450 nm, and the fluorescence decay observed for this species is effectively single-exponential with a decay time of 4.8 ns, which we attribute to the excited contact ion pair state, I*.

Interestingly, at 490 nm, the decay trace remained single-exponential at $w_0 = 0$ and 1, but at higher w_0 values, a distinct growth component in the fluorescent transients (∼0.4−0.6 ns) was clearly observed, although the relative contribution of the growth component was fairly low due to the shorter time constant of this component (∼0.4 ns) compared to that of the decay (∼5 ns) and also due to different overlapping emissions. However, the appearance of the growth component is consistent with the evolution of the tautomer emission of 7H4MC in TX-100 reverse micelles beyond $w_0 = 2$ and further confirms that the emission around 490 nm is due to the formation of the tautomer from the excited neutral dye within its excited-state lifetime. Since the tautomer formation takes place through a solvent-mediated intramolecular proton-transfer process, the tautomer can be formed only beyond $w_0 = 2$ in the TX-100 reverse micelles when the hydration of the oxyethylene chains of TX-100 is effectively saturated and the water pool formation begins in the reverse micelle. Due to the involvement of different hydrogen-bonded complexes and the contact ion pair states in addition to the usual neutral, anionic, and tautomeric forms, the detailed kinetic analysis in TX-100 reverse micelles becomes more complicated than that in BDHC and AOT reverse micelles. Nevertheless, it may be emphasized that the steady-state and time-resolved fluorescence results obtained in the present study provide many interesting insights about the evolution of the water pools in different reverse micelles and their effect on the possible photoinduced processes in the protopropic dye investigated in the present work.

4. Conclusions

The excited-state proton-transfer and the phototautomerization behaviors of 7H4MC dye have been investigated in cationic BDHC and nonionic TX-100 reverse micelles, and the results have been compared with those reported earlier in anionic AOT reverse micelles. The prototropic behavior of the dye clearly indicates that the microenvironment in the vicinity of the probe is largely different in the three reverse micelles considered. Although both the anionic and the tautomeric forms of 7H4MC are formed simultaneously from the excited neutral dye in AOT and BDHC reverse micelles, the results indicate that the anionic form of 7H4MC is more stabilized than the tautomer form at higher w_0 values in BDHC reverse micelles, though both of these forms are equally stable in the AOT reverse micelle. These differences have been attributed to the additional electrostatic stabilization experienced by the anionic form of the dye in BDHC reverse micelles due to the positively charged head groups of the surfactants. On the other hand, in nonionic TX-100 reverse micelles, the prototropic behavior of 7H4MC is much more complex than that in the ionic BDHC and AOT reverse micelles. Formation of new species like the contact ion pairs and hydrogen-bonded complexes of the dye with the surfactants is clearly observed in TX-100 reverse micelles, which are not indicated in the ionic reverse micelles. Surprisingly, in TX-100 reverse micelles, the anionic form of the dye is not very noticeable. This is inferred to be due to the different nature of the entrapped water in TX-100 reverse micelles than that in other micelles. It is indicated that up to $w_0 \sim 2$, the water added to the TX-100 reverse micelle is almost solely utilized to hydrate the oxyethylene chains of the surfactant, and only beyond $w_0 \sim 2$ does a water-pool-like structure start to form. However, the observed results indicate that even above $w_0 \sim 2$, the water pool in TX-100 reverse micelles is not as well defined as that in the ionic reverse micelles. As a result, the anionic form of the dye cannot be stabilized appreciably in the TX-100 reverse micelles. Interestingly, however, the formation of the tautomer species from the excited neutral dye is clearly detected beyond $w_0 \sim 2$. The present investigation on the prototropic behavior of the dye, 7H4MC, in different reverse micelles thus helps us to obtain many interesting insights into the evolution of the water pools in these reverse micelles and to understand their role in modulating the photoinduced processes in the prototropic dye 7H4MC. Grossly, it is indicated that the TX-100 reverse micelles behave in a completely different manner than the BDHC and AOT reverse micelles in relation to the excited-state behavior of a prototropic dye.

Acknowledgment. The authors are thankful to Dr. S. Nath for many fruitful discussions. Thanks are also due to Dr. S. K. Sarkar, Head, RPCD, BARC, and Dr. T. Mukherjee, Director, CG, BARC, for their constant encouragement and support.

References and Notes

(1) Pal, S. K.; Zewail, A. H. *Chem. Rev.* **2004**, *104*, 2099–2123.

(2) Nandi, N.; Bhattacharyya, K.; Bagchi, B. *Chem. Rev.* **2000**, *100*, 2013–2045.
(3) Prabhu, N.; Sharp, K. *Chem. Rev.* **2006**, *106*, 1616–1623.
(4) Bagchi, B. *Chem. Rev.* **2005**, *105*, 3197–3219.
(5) *Reverse Micelles*; Luisi, P. L., Straub, B., Eds.; Plenum Press: New York, 1984.
(6) Kalyanasundaram, K. *Photochemistry in Microheterogeneous Systems*; Academic Press: London, 1987.
(7) Luisi, P. L.; Giomini, M.; Pileni, M. P.; Robinson, B. H. *Biochim. Biophys. Acta* **1988**, *947*, 209–246.
(8) Jain, T. K.; Varshney, T. K.; Maitra, A. *J. Phys. Chem.* **1989**, *93*, 7409–7414.
(9) Wong, M.; Thomas, J. K.; Novak, T. *J. Am. Chem. Soc.* **1977**, *99*, 4730–4736.
(10) Hasegawa, M.; Sugimura, T.; Suzaki, Y.; Shindo, Y. *J. Phys. Chem.* **1994**, *98*, 2120–2124.
(11) Faeder, J.; Ladanyi, B. M. *J. Phys. Chem. B* **2000**, *104*, 1033–1046.
(12) Borsarelli, C. D.; Cosa, J. J.; Previtali, C. M. *Langmuir* **1993**, *9*, 2895–2901.
(13) Moilanen, D. E.; Levinger, N. E.; Spry, D. B.; Fayer, M. D. *J. Am. Chem. Soc.* **2007**, *129*, 14311–14318.
(14) Piletic, I. R.; Moilanen, D. E.; Spry, D. B.; Levinger, N. E.; Fayer, M. D. *J. Phys. Chem. A* **2006**, *110*, 4985–4999.
(15) Cohen, B.; Huppert, D.; Solnstev, K. M.; Tsafadia, Y.; Nachliel, E.; Gutman, M. *J. Am. Chem. Soc.* **2002**, *124*, 7539–7547.
(16) Bardez, E.; Monnier, E.; Valeur, B. *J. Phys. Chem.* **1985**, *89*, 5031–5036.
(17) Bardez, E.; Goguillon, B.-T.; Keh, E.; Valeur, B. *J. Phys. Chem.* **1984**, *88*, 1909–1913.
(18) Andrade, S. M.; Costa, S. M. B.; Pansu, R. *Photochem. Photobiol.* **2000**, *71*, 405–412.
(19) Angulo, G.; Oganero, J. A.; Carranza, M. A.; Douhal, A. *J. Phys. Chem. B* **2006**, *110*, 24231–24237.
(20) Douhal, A.; Angulo, G.; Gil, M.; Organero, J. A.; Sanz, M.; Tormo, L. *J. Phys. Chem. B* **2007**, *111*, 5487–5493.
(21) Dutta Choudhury, S.; Nath, S.; Pal, H. *J. Phys. Chem. B* **2008**, *112*, 7748–7753.
(22) Moriya, T. *Bull. Chem. Soc. Jpn.* **1983**, *56*, 6–14.
(23) Moriya, T. *Bull. Chem. Soc. Jpn.* **1988**, *61*, 1873–1886.
(24) Cohen, B.; Huppert, D. *J. Phys. Chem. A* **2001**, *105*, 7157–7164.
(25) Cohen, B.; Huppert, D. *J. Phys. Chem. A* **2002**, *106*, 1946–1955.
(26) Trozzolo, A. M.; Dienes, A.; Shank, C. V. *J. Am. Chem. Soc.* **1974**, *96*, 4699–4700.
(27) Shank, C. V.; Dienes, A.; Trozzolo, A. M.; Myer, J. A. *Appl. Phys. Lett.* **1970**, *16*, 405–407.
(28) Dienes, A.; Shank, C. V. *Appl. Phys. Lett.* **1970**, *17*, 189–191.
(29) Georgieva, I.; Trendafilova, N.; Aquino, A.; Lischka, H. *J. Phys. Chem. A* **2005**, *109*, 11860–11869.
(30) Georgieva, I.; Trendafilova, N.; Aquino, A. J. A.; Lischka, H. *J. Phys. Chem. A* **2007**, *111*, 127–135.
(31) Kobayashi, T. *J. Phys. Chem.* **1978**, *82*, 2277–2281.
(32) Seixas de Melo, J.; Maçanita, A. L. *Chem. Phys. Lett.* **1993**, *204*, 556–562.
(33) Abdel Mottaleb, M. S. A.; El-sayed, B. A.; Abo-Aly, M. M.; El-Kady, M. Y. *J. Photochem. Photobiol., A* **1989**, *46*, 379–390.
(34) Bardez, E.; Boutin, P.; Valeur, B. *Chem. Phys. Lett.* **1992**, *191*, 142–148.
(35) Seixas de Melo, J.; Fernandes, P. F. *J. Mol. Struct.* **2001**, *565*−*566*, 69–78.
(36) Yakatan, G. J.; Juneau, R. J.; Schulman, S. G. *Anal. Chem.* **1972**, *44*, 1044–1046.
(37) Schulman, S. G.; Rosenberg, L. S. *J. Phys. Chem.* **1979**, *83*, 447–451.
(38) Hoshiyama, M.; Kubo, K.; Igarashi, T.; Sakurai, T. *J. Photochem. Photobiol., A* **2001**, *138*, 227–233.
(39) Zhu, D.-M.; Wu, X.; Schelly, Z. A. *Langmuir* **1992**, *1992*, 1538–1540.
(40) McNeil, R.; Thomas, J. K. *J. Colloid Interface Sci.* **1981**, *83*, 57–65.
(41) Correa, N. M.; Biasutti, M. A.; Silber, J. J. *J. Colloid Interface Sci.* **1996**, *184*, 570–578.
(42) Grand, D.; Dokutachev, A. *J. Phys. Chem. B* **1997**, *101*, 3181–3186.
(43) Zhu, D.-M.; Schelly, Z. A. *J. Phys. Chem.* **1992**, *96*, 7121–7126.
(44) Dutt, G. B. *J. Phys. Chem. B* **2004**, *108*, 7944–7949.
(45) O'Connor, D. V.; Philips, D. *Time-Correlated Single Photon Counting*; Academic Press: London, 1984.
(46) Lakowicz, J. R. *Principles of Fluorescence Spectroscopy*, 3rd ed.; Springer: New York, 2006.
(47) Giestas, L.; Yihwa, C.; Lima, J. C.; Vautier-Giongo, C.; Lopes, A.; Maçanita, A. L.; Quina, F. H. *J. Phys. Chem. A* **2003**, *107*, 3263–3269.
(48) Andrade, S. M.; Costa, S. M. B. *Photochem. Photobiol. Sci.* **2002**, *2002*, 500–506.

JP8111759